Chemistry – A European Journal

ChemEurJ Chemistry Europe
European Chemical Societies Publishing

RESEARCH ARTICLE OPEN ACCESS

Catalyst-Free Selective Reduction of Nitrogen Dioxide to Nitric Oxide

Awais W. Seyyad | Agamemnon E. Crumpton | Reece Lister-Roberts | Meera Mehta

Department of Chemistry, University of Oxford, Oxford, UK

Correspondence: Meera Mehta (meera.mehta@chem.ox.ac.uk)

Received: 18 April 2026 | **Revised:** 28 May 2026 | **Accepted:** 2 June 2026

Keywords: catalyst-free | main group chemistry | nitric oxide | nitrogen dioxide | reduction

ABSTRACT

Nitrogen dioxide (NO_2) is a highly toxic gas and a notorious respiratory irritant that contributes to the greenhouse effect and acid rain. Herein, we study the catalyst-free reduction of NO_2 with boranes, silanes, and the hydrogen surrogates 1,4-cyclohexadiene and isopropyl alcohol, resulting in the selective formation of nitric oxide (NO). Selective NO generation was confirmed by electron paramagnetic resonance spectroscopy and low-temperature $^{15}N\{^1H\}$ nuclear magnetic resonance spectroscopy. Additionally, density functional theory calculations have been employed to probe the mechanism of these reductions.

1 | Introduction

Combustion engines are pervasive in industry and transportation, and at elevated temperatures, they generate nitrogen oxides, namely nitrogen dioxide (NO_2) and nitric oxide (NO). The generation of NO_2 is particularly undesirable due to its deleterious environmental and health effects [1]. Exposure to NO_2 has been associated with increased mortality and heightened susceptibility to cardiovascular and respiratory disease [2]. Additionally, NO_2 has been implicated in the formation of tropospheric ozone [3], photochemical smog [4], acid rain [5], and the indirect enhancement of the greenhouse effect [6]. Current technologies that degrade NO_x emissions require the use of noble metal catalytic converters [7]. These catalysts operate at elevated temperatures (> 200 °C) and rely on scarce, expensive, and depleting transition metals.

NO_2 can be degraded by single-electron reduction to nitrite salts or nitrous acid (HONO), or via a two-electron reduction to NO (Figure 1). In contrast to NO_2, NO is considerably less toxic and is stable *in vivo* [8]. NO plays a critical role as a biochemical signaling molecule, responsible for mediating a wide array of physiological responses. Mineral aerosol substrates [9, 10], polycyclic aromatic hydrocarbons [11], and hydrated bulk minerals [12] are all known to mediate single-electron pathways for NO_2 degradation, while two-electron pathways are less widely explored. In 2012, Mullins reported the complete and selective reduction of NO_2 to NO on hydrogen-precovered Au at cryogenic temperatures [13]. Later, in 2021, Grützmacher reported a homogeneous Rh(I)–Pt(II) based heterobimetallic catalyst capable of hydrogenating NO_x gases, including NO_2 [14]. Furthermore, a recent report by Chen and co-workers illustrates how mixtures of oxalic acid and Fe_2O_3 can also facilitate this transformation [15]. There has been global interest in developing catalyst-free protocols as sustainable alternatives to transition-metal mediated processes. Herein, we study the reactivity of organo-main group reductants, including boranes, silanes, cyclohexadiene, and isopropyl alcohol, with NO_2 in the absence of a catalyst and demonstrate the selective production of NO.

2 | Results and Discussion

First, excess NO_2 (~1 atm, 25°C) was added to a degassed C_6D_6 solution of 4,4,5,5-tetramethyl-1,3,2-dioxaborolane (HBpin), yielding an orange solution. Rapid gas evolution was observed, and the reaction mixture gradually turned green over the course

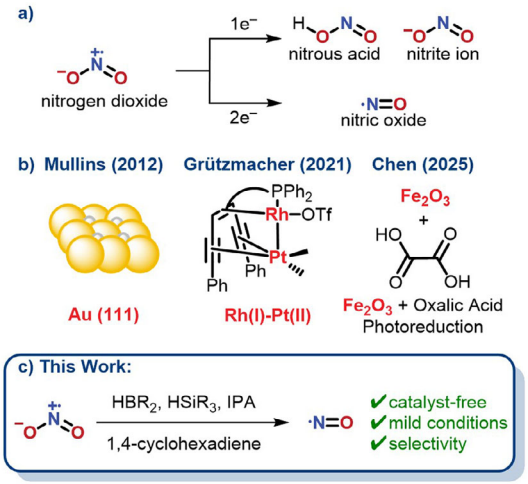

FIGURE 1 | (a) Products from NO_2 reduction. (b) Transition metal-mediated reductions of NO_2. (c) This work, catalyst-free reduction of NO_2 by main group reductants.

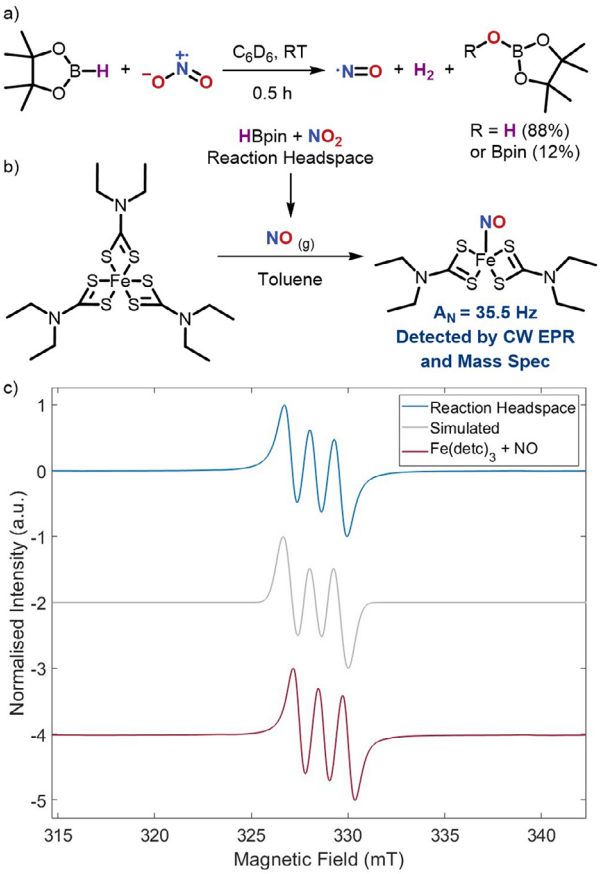

FIGURE 2 | (a) Reduction of NO_2 with HBpin. (b) Spin trapping of NO by [Fe(detc)$_3$] to generate the EPR active species [Fe(NO)(detc)$_2$]. (c) Experimental CW EPR spectrum of spin-trapped NO by [Fe(detc)$_3$] at room temperature (experimental parameters: solvent: toluene, frequency: 9.367292 GHz, receiver gain: 30 dB, g = 2.038, blue). Simulation of experimental CW EPR spectrum (1 x A_N = 35.5 Hz) (grey). CW EPR spectrum of independently synthesized [Fe(NO)(detc)$_2$] from the reaction [Fe(detc)$_3$] with NO at room temperature (experimental parameters: solvent: toluene, frequency: 9.372613 GHz, receiver gain: 30 dB, g = 2.038, red).

of 5 min. Freezing the reaction mixture in liquid nitrogen (−196°C) after 5 min resulted in the formation of a bright blue solid. The observed thermochromism is consistent with the formation of dinitrogen trioxide (N_2O_3), a known product formed from NO and NO_2 coupling [16, 17]. After 30 min, the reaction mixture was analyzed by ^{1}H and ^{11}B{^{1}H} NMR spectroscopy, which revealed the complete consumption of HBpin and formation of HOBpin and pinBOBpin (88% and 12%, respectively, by ^{1}H NMR using toluene as an internal standard) and H_2 (Figure 2). The reaction mixture was then cooled to −20°C, to freeze any residual NO_2 (which has a melting point of −11.2°C) [17], and the remaining volatile products were vacuum transferred to an electron paramagnetic resonance (EPR) tube. Initially, no resonances could be detected by EPR spectroscopy at room temperature or −123°C (150 K). A separate control experiment of only NO_2 in C_6D_6 confirmed that NO_2 gives rise to an EPR resonance as a broad singlet at g = 2.001. Following the addition of excess HBpin to a solution of NO_2, no resonances could be detected by EPR spectroscopy, indicating the complete consumption of NO_2. It has previously been reported that it can be challenging to directly observe NO by EPR spectroscopy, due to rapid spin relaxation arising from large spin-orbit coupling and collisional broadening effects associated with gaseous radicals [18, 19]. Thus, the reaction was repeated as initially described and, after freezing the solution, the headspace was transferred to an EPR tube containing a solution of [Fe(detc)$_3$] (detc = diethyldithiocarbamate), a known NO spin trap [20]. Analysis of this reaction mixture by continuous wave (CW) EPR spectroscopy successfully detected the EPR active complex [Fe(NO)(detc)$_2$]. Additionally, known NO trapping reagent [T(O-Me)PP(Co)] was employed in a similar manner to further confirm the generation of NO. Analysis of the reaction mixture by ^{1}H NMR spectroscopy confirmed the formation of [T(O-Me)PP(Co)(NO)], as expected (see Section S6.2). These experiments confirm the formation of NO in the headspace when HBpin is allowed to react with NO_2.

Isotopically labelled $^{15}NO_2$ was generated by reacting ^{15}N-labelled nitric acid with elemental copper [21]. The gaseous product was then vacuum transferred to a separate ampoule and repeatedly degassed to remove any traces of ^{15}NO (see Sections S5 and S8). A degassed solution of HBpin in d_8-toluene was then pressurized with $^{15}NO_2$, and was allowed to react at room temperature for 10 min. The reaction mixture was then cooled to −50°C, at which point a distinct blue color was observed. The reaction mixture was subsequently analyzed by ^{15}N{^{1}H} NMR spectroscopy at −50°C. At this temperature, NO_2 is known to dimerize to form the diamagnetic product N_2O_4. Additionally, the diamagnetic adduct of NO and NO_2, N_2O_3, is also known to form. It is worth noting that the dimer of NO, N_2O_2, is significantly weaker and more unstable [22], and thus was not anticipated to be detectable by NMR spectroscopy in these experiments. Low-temperature ^{15}N{^{1}H} NMR spectroscopy confirmed the presence of N_2O_3 with two broad resonances at 671 and 439 ppm, and N_2O_4 at 360 ppm (Figure 3). Upon warming to room temperature, no resonances could be detected by ^{15}N{^{1}H} NMR spectroscopy, in line with the formation of diamagnetic adducts at low temperature as opposed to persistent diamagnetic species. These experiments also show that NO_2 and NO, along with their corresponding dimers at low temperature, are the only nitrogen-containing

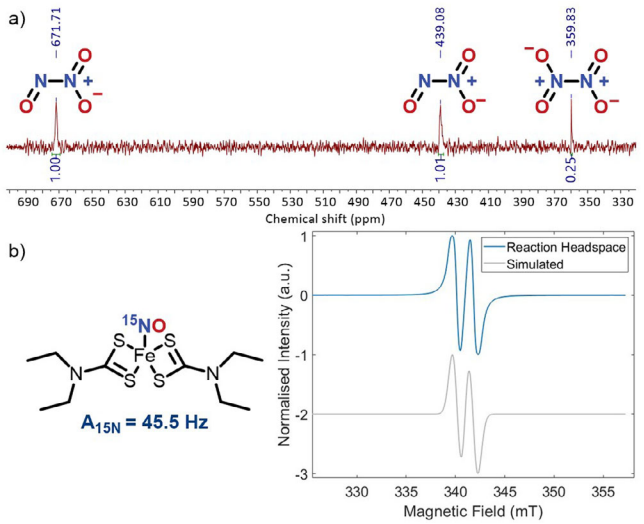

FIGURE 3 | (a) Low-temperature (−50°C) $^{15}N\{^1H\}$ NMR spectrum showing N_2O_3 and N_2O_4. (b) Spin trapping of ^{15}NO and CW EPR spectrum at room temperature (experimental parameters: solvent: toluene, frequency: 9.739740 GHz, receiver gain: 30 dB, g = 2.038, blue) and simulation of $[Fe(^{15}NO)(detc)_2]$ (1 x A_N = 45.5 Hz, grey).

products in the reaction mixture. The reaction mixture was allowed to react for a further 15 min at room temperature, after which it was cooled to −50°C and reanalyzed by $^{15}N\{^1H\}$ NMR spectroscopy. No resonances could be detected, suggesting the complete hydroborative reduction of $^{15}NO_2$ to ^{15}NO. The reaction headspace was vacuum transferred to a J-Young EPR tube charged with a solution of $[Fe(detc)_3]$ in toluene, and EPR spectroscopy again confirmed the formation of $[Fe(^{15}NO)(detc)_2]$ (with a distinct N hyperfine coupling x1 A_N = 45.5 Hz), the ^{15}NO spin trapped product. The larger hyperfine coupling is in agreement with ^{15}N's larger gyromagnetic ratio [23].

In order to gain insight into the mechanism, several pathways were postulated and computationally assessed using r^{2}SCAN-3c composite method with conductor-like polarizable continuum model (CPCM) benzene solvation. Given the radical nature of NO_2, single-electron mechanisms were considered. However, mechanisms involving H atom abstraction or the homolytic cleavage of HBpin were found to be energetically inaccessible (see Section S9.1). Furthermore, experimental observations indicate that pathways involving $^{\bullet}$Bpin are unlikely, as evidenced by B_2pin_2 showing no reaction with NO_2. Thus, two-electron hydride mechanisms were explored computationally. Figure 4 summarizes a computationally viable mechanism, with adduct formation between NO_2 and HBpin being rate-determining to yield **Int-1**. Next, **Int-1** can rearrange into **TS-2** in a near-barrierless fashion, followed by hydride migration to give HOBpin and NO via **TS-3**. Following on from **Int-1**, both three- and five-membered transition states were also considered and discounted due to their higher energetic barriers (See Sections S9.2 and S9.3).

Since both HOBpin, pinBOBpin, and H_2 are observed in the reaction mixture, we postulated that HOBpin could react with excess HBpin in the reaction mixture to give pinBOBpin and H_2. However, when independently synthesized HOBpin was reacted with one equivalent of HBpin in C_6D_6, no reaction was observed at room temperature over the course of a day. Furthermore, the direct dehydrocoupling between HOBpin and HBpin was computed to be prohibitively high (**TS-4'** $\Delta G^{\ddagger}$ = 45.3 kcal mol^{-1}). Although, it should be noted that analogous dehydrocoupling reactions can be mediated by Brønsted-Lowry bases or Lewis acids [24–28], and thus these pathways cannot be completely ruled out. Nonetheless, we considered a separate mechanism

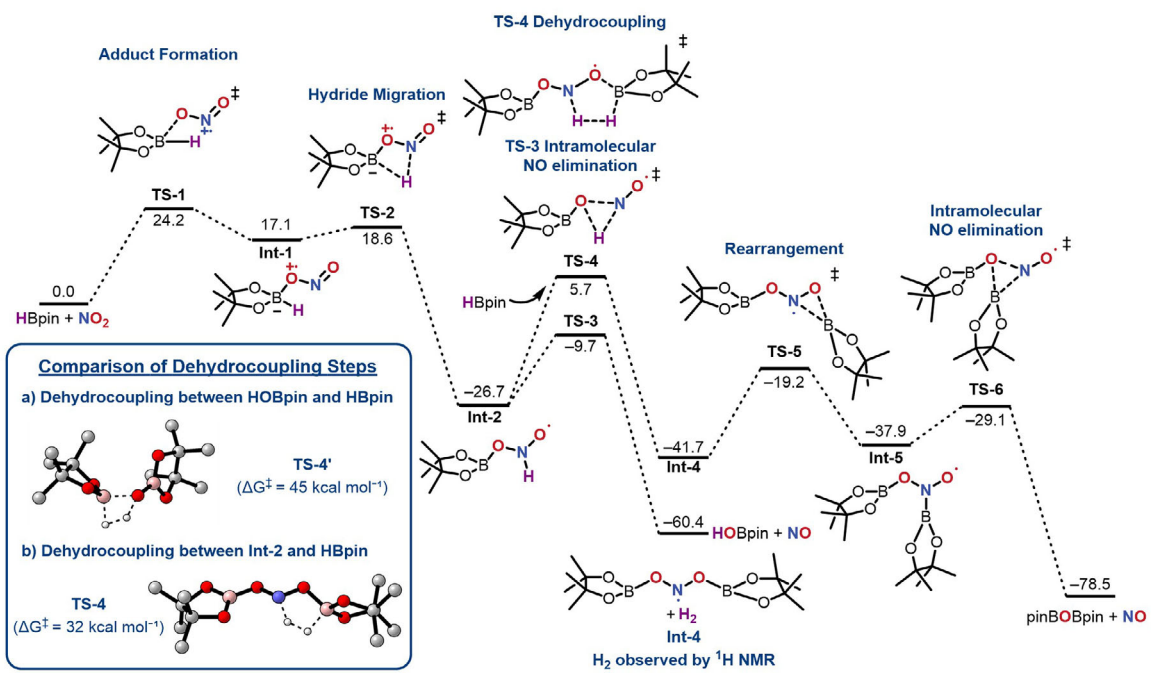

FIGURE 4 | Calculated reaction pathway for the formation of HOBpin, pinBOBpin, and H_2 gas from the reduction of NO_2 with HBpin. Gibbs energies in kcal mol^{-1} (r^{2}SCAN-3c composite method with CPCM benzene solvation). Intermediates have been drawn as Lewis structures, with spin density calculations provided in Section S9.5.

TABLE 1 | Scope of main group reductants tested in the catalyst-free reduction of NO_2.

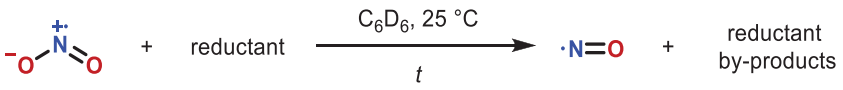

Reductant	*t*	Reductant consumption (%)[a]
HBpin	30 min	100
B_2pin_2	12 h	0
Et_3SiH	4 h	84
Ph_3SiH	12 h	74
Si_2Me_6	12 h	0
CHD	5 min	100
IPA	12 h	100

[a]Determined by ^{1}H NMR spectroscopy using toluene as an internal standard. CHD = 1,4-cyclohexadiene; IPA = isopropyl alcohol.

which could lead to the formation of pinBOBpin and H_2 (shown in Figure 4). Instead, **Int-2** can react with a second equivalent of HBpin via **TS-4** ($\Delta G^{\ddagger}$ = 32 kcal mol^{-1}) to give **Int-4**, a diborylated aminyl-type radical, together with H_2. The relatively high barrier is consistent with the observed selective formation of HOBpin over pinBOBpin in this reaction (88% vs. 12%).

Next, various main group reducing agents were screened to probe the generality of this method. $HB(C_6F_5)_2$, catecholborane, and ammonia-borane were tested and found to yield a complex mixture of products consistent with decomposition products. While triethylsilane (Et_3SiH) was found to react in an analogous fashion to HBpin, albeit not to completion, affording Et_3SiOH (74%) and $Et_3SiOSiEt_3$ (10%) over the course of 4 h (Table 1). Triphenylsilane (Ph_3SiH) displayed similar reactivity, forming only Ph_3SiOH (74%) after 12 h. Whereas reaction of hexamethyldisilane (Si_2Me_6) with NO_2 showed no reaction even after 12 h. Hydrogen-transfer reagents were also investigated; these reagents are attractive reductants as they bypass the safety hazards associated with using flammable $H_{2(g)}$ [29, 30]. A degassed solution of 1,4-cyclohexadiene (CHD) in C_6D_6 was reacted with excess NO_2 (~1 atm, 25°C), resulting in the immediate formation of a persistent bright green solution. ^{1}H and $^{13}C\{^1H\}$ NMR spectroscopy confirmed the clean and quantitative conversion of 1,4-cyclohexadiene to benzene. No other organic products were detected by ^{1}H or $^{13}C\{^1H\}$ NMR spectroscopy. Water was not observed in the ^{1}H NMR spectrum; however, a broad signal at ~6 ppm was detected, in line with the expected resonance of nitrous acid (HONO) [31], possibly formed by water reacting with N_2O_3 [16]. Spin trapping experiments using [Fe(detc)$_3$] again confirmed the generation of NO from this reaction mixture. EPR spectroscopy was employed to assess whether the final reduction product was NO or HONO. HONO is known to be unstable and decomposes into NO_2, NO, and water. If HONO were the final reduction product, we postulated that the regeneration of NO_2 would be observable by CW EPR spectroscopy. Thus, an EPR tube charged with a solution of excess 1,4-cyclohexadiene in C_6D_6 was degassed and pressurized with NO_2. The reaction was monitored daily by EPR spectroscopy, and regenerated NO_2 was not detected over the course of one week. Therefore, it is likely that 1,4-cyclohexadiene reacts with NO_2 to give HONO as an intermediate, which is then further reduced to NO. Both radical and proton-hydride mechanisms were probed computationally, and proton-hydride step-wise transfer mechanisms were found to be energetically infeasible (see Section S9.6).

Figure 5 presents a plausible single-electron transfer mechanism for how 1,4-cyclohexadiene reduces NO_2. Significant radical spin density in NO_2 is located on the N atom [32, 33], which can abstract a H$^{\bullet}$ from 1,4-cyclohexadiene to give O(H)NO (**Int-7**) via **TS-7**, which is slightly more energetically favorable than **TS-7'**. Intramolecular isomerization of ON(H)O to HONO was found to be kinetically disfavored (see Section SS9.7, **TS-d**: $\Delta G^{\ddagger}$ = 47.2 kcal mol^{-1}). However, isomerization via a six-membered intermolecular transition state, **TS-8**, is energetically feasible and converts **Int-7** to HONO (**Int-8**). Finally, HONO reacts with cyclohexadienyl radical to afford NO, benzene, and water. This computed mechanism is in agreement with Mullins' gold-mediated hydrogenation mechanism, where hydrogen atoms first reduce NO_2 to HONO, which is then further reduced to NO [13].

Isopropyl alcohol (IPA) was also tested as a hydrogen-transfer reductant. When reacted with excess NO_2, IPA was fully consumed within 12 h, forming only acetone (27%) and isopropyl nitrite (73%), confirmed by ^{1}H and $^{13}C\{^1H\}$ NMR spectroscopy. A broad resonance at ~6 ppm was again observed in the ^{1}H NMR spectrum, suggesting HONO as an intermediate. Furthermore, the formation of isopropyl nitrite is consistent with the presence of HONO in the reaction mixture [34]. Additionally, N_2O_3 (the NO_2 and NO adduct) is also known to be an active nitrosating agent for alkyl alcohols [35]. Spin trapping experiments using Fe(detc)$_3$confirmed the formation of NO when IPA was employed as a reductant.

3 | Conclusion

In summary, we report the selective reduction of NO_2 to NO using common main group reducing agents, including boranes, silanes, and hydrogen-transfer reagents, in a catalyst-free manner. Selective NO formation was confirmed by EPR studies, including the use of NO-trapping reagents, and labelled ^{15}N NMR experiments. The mechanisms for these reductions were investigated

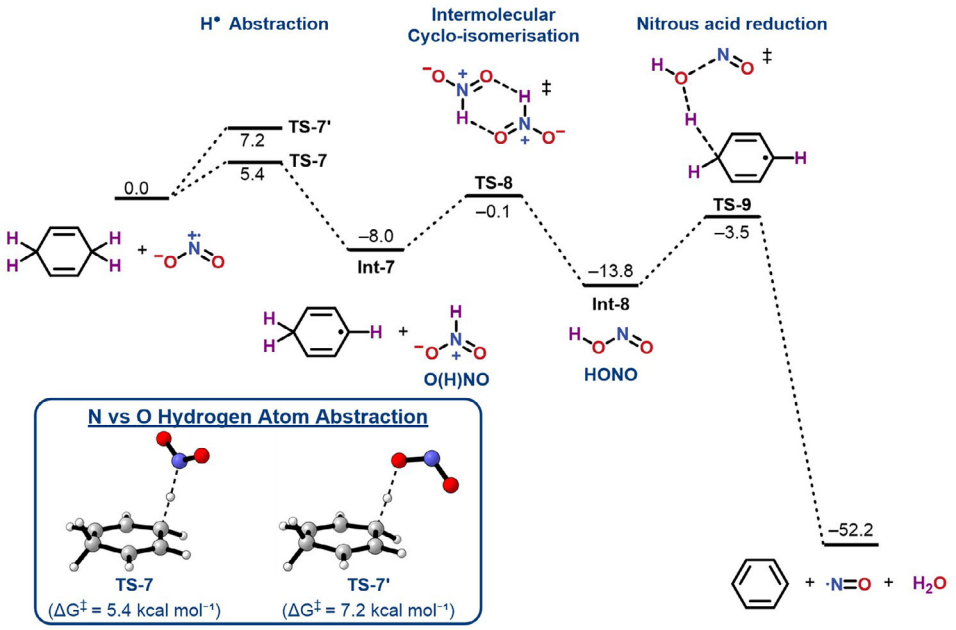

FIGURE 5 | Calculated reaction pathway for the reduction of NO_2 by 1,4-cyclohexadiene. Gibbs energies in kcal mol^{-1} (r^2SCAN-3c composite method with CPCM benzene solvation).

computationally. The borane and silane mediated pathways are believed to differ from those involving hydrogen-transfer reagents such as 1,4-cyclohexadiene and isopropyl alcohol, with the latter possibly proceeding via HONO as an intermediate.

Acknowledgments

We thank the University of Oxford and UKRI (EP/Y037391/1) for supporting M.M., A.W.S., R.L.-R., and A.E.C. We thank Dr. Bono van IJzendoorn for useful discussions around NO_2 gas generation, Dr. Nick Rees for support with NMR studies, and Dr. William Myers for advice about NO spin trapping, EPR spectrometer assistance, and related discussions.

Conflicts of Interest

The authors declare no conflicts of interest.

Data Availability Statement

The data that supports the findings of this study are available in the supplementary material of this article.

References

1. T.-M. Chen, W. G. Kuschner, J. Gokhale, and S. Shofer, "Outdoor Air Pollution: Nitrogen Dioxide, Sulfur Dioxide, and Carbon Monoxide Health Effects," *American Journal of the Medical Sciences* 333 (2007): 249–256.

2. S. Huang, H. Li, M. Wang, et al., "Long-Term Exposure to Nitrogen Dioxide and Mortality: A Systematic Review and Meta-Analysis," *Science of The Total Environment* 776 (2021): 145968.

3. D.-H. Nguyen, C. Lin, C.-T. Vu, et al., "Tropospheric Ozone and NOx: A Review of Worldwide Variation and Meteorological Influences," *Environmental Technology & Innovation* 28 (2022): 102809.

4. A. W. Brewer, C. T. McElroy, and J. B. Kerr, "Nitrogen Dioxide Concentrations in the Atmosphere," *Nature* 246 (1973): 129–133.

5. F. Menezes and G. M. Popowicz, "Acid Rain and Flue Gas: Quantum Chemical Hydrolysis of NO," *ChemPhysChem* 23 (2022): e202200395.

6. G. Lammel and H. Graßl, "Greenhouse Effect of NOX," *Environmental Science and Pollution Research* 2 (1995): 40–45.

7. S. Bhattacharyya and R. K. Das, "Catalytic Control of Automotive NOx: A Review," *International Journal of Energy Research* 23 (1999): 351–369.

8. L. B. Maia and J. J. G. Moura, "How Biology Handles Nitrite," *Chemical Reviews* 114 (2014): 5273–5357.

9. X. Gao, C. Zhong, M. Tang, Q. Ma, and C. Liu, "Key Factors Determining Heterogeneous Uptake Kinetics of NO2 Onto Alumina: Implication for the Linkage between Laboratory Work and Modeling Study," *Journal of Geophysical Research: Atmospheres* 126 (2021): e2021JD034694.

10. M. Ndour, B. D'Anna, C. George, et al., "Photoenhanced Uptake of NO2 on Mineral Dust: Laboratory Experiments and Model Simulations," *Geophysical Research Letters* 35 (2008): L05812.

11. J. Liu, B. Li, H. Deng, et al., "Resolving the Formation Mechanism of HONO via Ammonia-Promoted Photosensitized Conversion of Monomeric NO2 on Urban Glass Surfaces," *Journal of the American Chemical Society* 145 (2023): 11488–11493.

12. Z. Liu, A. Sinopoli, J. S. Francisco, and I. Gladich, "Water-Catalyzed Formation of Reactive Oxygen Species From NO2 on a Weakly Hydrated Calcite Surface," *Journal of the American Chemical Society* 146 (2024): 17898–17907.

13. M. Pan, H. C. Ham, W.-Y. Yu, G. S. Hwang, and C. B. Mullins, "Highly Selective, Facile NO2 Reduction to NO at Cryogenic Temperatures on Hydrogen Precovered Gold," *Journal of the American Chemical Society* 135 (2013): 436–442.

14. P. Jurt, A. S. Abels, J. J. Gamboa-Carballo, et al., "Reduction of Nitrogen Oxides by Hydrogen With Rhodium(I)–Platinum(II) Olefin Complexes as Catalysts," *Angewandte Chemie International Edition* 60 (2021): 25372–25380.

15. X. Chen, H. Jiang, J. Chen, et al., "Oxalate-Bridged Binuclear Fe(II) Drives Concerted Two-Electron Reduction of NO2 by Substantial Spin Interactions," *Angewandte Chemie International Edition* 65 (2026): e12391.

16. K. A. Rosadiuk and D. S. Bohle, "Anhydrous Dinitrogen Trioxide Solutions for Brønsted Acid Free Nitrous Acid Chemistry," *European Journal of Inorganic Chemistry* 2017 (2017): 5461–5465.

17. P. Gray and A. D. Yoffe, "The Reactivity and Structure of Nitrogen Dioxide," *Chemical Reviews* 55 (1955): 1069–1154.

18. M. Mendt and A. Pöppl, "The Line Width of the EPR Signal of Gaseous Nitric Oxide as Determined by Pressure and Temperature-Dependent X-band Continuous Wave Measurements," *Applied Magnetic Resonance* 46 (2015): 1249–1263.

19. R. S. da Silva, M. Y. Ballester, L. R. Ventura, and C. E. Fellows, "Theoretical Study of the Spin-Orbit Coupling in the X2Π state of NO," *Chemical Physics Letters* 780 (2021): 138896.

20. S. Fujii and T. Yoshimura, "A New Trend in Iron–Dithiocarbamate Complexes: As an Endogenous NO Trapping Agent," *Coordination Chemistry Reviews* 198 (2000): 89–99.

21. R. Que, W. Ding, S. Sha, and A. Simple, "Facile Demonstration of Copper and Nitric Acid Reaction," *Journal of Chemical Education* 99 (2022): 2762–2765.

22. S. G. Kukolich, "The Structure of the Nitric Oxide Dimer," *Journal of the American Chemical Society* 104 (1982): 4715–4716.

23. A. H. Beth, S. D. Venkataramu, K. Balasubramanian, et al., "15N- and 2H-Substituted Maleimide Spin Labels: Improved Sensitivity and Resolution for Biological EPR Studies," *Proceedings of the National Academy of Sciences* 78 (1981): 967–971.

24. D. J. Liptrot, M. S. Hill, M. F. Mahon, and A. S. S. Wilson, "Alkaline-Earth-Catalyzed Dehydrocoupling of Amines and Boranes," *Angewandte Chemie International Edition* 54 (2015): 13362–13365.

25. A. A. Toutov, K. N. Betz, M. C. Haibach, A. M. Romine, and R. H. Grubbs, "Sodium Hydroxide Catalyzed Dehydrocoupling of Alcohols With Hydrosilanes," *Organic Letters* 18 (2016): 5776–5779.

26. L. Wu, V. T. Annibale, H. Jiao, A. Brookfield, D. Collison, and I. Manners, "Homo- and Heterodehydrocoupling of Phosphines Mediated by Alkali Metal Catalysts," *Nature Communications* 10 (2019): 2786.

27. J. M. Blackwell, K. L. Foster, V. H. Beck, and W. E. Piers, "B(C6F5)3-Catalyzed Silation of Alcohols: A Mild, General Method for Synthesis of Silyl Ethers," *Journal of Organic Chemistry* 64 (1999): 4887–4892.

28. M. Pérez, C. B. Caputo, R. Dobrovetsky, and D. W. Stephan, "Metal-Free Transfer Hydrogenation of Olefins via Dehydrocoupling Catalysis," *Proceedings of the National Academy of Sciences* 111 (2014): 10917.

29. M. Mehta and J. M. Goicoechea, "Nitrenium Salts in Lewis Acid Catalysis," *Angewandte Chemie International Edition* 59 (2019): 2715–2719.

30. A. Baschieri, R. Amorati, L. Valgimigli, and L. Sambri, "1-Methyl-1,4-Cyclohexadiene as a Traceless Reducing Agent for the Synthesis of Catechols and Hydroquinones," *Journal of Organic Chemistry* 84 (2019): 13655–13664.

31. A. V. Marchenko, A. N. Vedernikov, D. F. Dye, M. Pink, J. M. Zaleski, and K. G. Caulton, "An Electron-Excessive Nitrosyl Complex: Reactivity of a Ligand-Centered Radical Leading to Coordinated HNO," *Inorganic Chemistry* 41 (2002): 4087–4089.

32. C. R. Brundle, D. Neumann, W. C. Price, D. Evans, A. W. Potts, and D. G. Streets, "Electronic Structure of NO2 Studied by Photoelectron and Vacuum-UV Spectroscopy and Gaussian Orbital Calculations," *Journal of Chemical Physics* 53 (1970): 705–715.

33. P. W. Atkins, N. Keen, and M. C. R. Symons, "561. Oxides and Oxyions of the Non-Metals. Part II. CO2– and NO2," *Journal of the Chemical Society* (1962): 2873–2880.

34. J. M. González-Sánchez, M. Huix-Rotllant, N. Brun, et al., "Direct Formation of HONO Through Aqueous-Phase Photolysis of Organic Nitrates," *Atmospheric Chemistry and Physics* 23 (2023): 15135–15147.

35. L. Grossi and S. Strazzari, "A New Synthesis of Alkyl Nitrites: the Reaction of Alkyl Alcohols With Nitric Oxide in Organic Solvents," *Journal of Organic Chemistry* 64 (1999): 8076–8079.

Supporting Information

Additional supporting information can be found online in the Supporting Information section.

Supporting File 1 : The data supporting this article have been included as part of the Supplementary Information (.pdf).